ACOUSTIC EMISSIONS IN TENSILE FRACTURES

by

GERASIMOS CHOULIARAS

Department of Geophysics

submitted in partial fulfillment
of the requirement for the degree of Bachelor of Science

Faculty of Science
The University of Western Ontario
London, Canada
1981

ACOUSTIC EMISSIONS IN TENSILE FRACTURES

by

GERASIMOS CHOULIARAS

Department of Geophysics

submitted in partial fulfillment
of the requirement for the degree of Bachelor of Science

Faculty of Science
The University of Western Ontario
London, Canada
1981

A B S T R A C T

This study is concerned with the monitoring of the acoustic emission activity associated with the formation of three types of tensile fractures in glass plates.

The rate of occurrence and the amplitudes of the acoustic emissions are observed to be dependant on the nature of applied stress at the fracture tip.

It is deduced that acoustic emission patterns observed in controlled modelling experiments involving tensile fractures are analogous to precursory seismicity patterns.

ACKNOWLEDGMENTS

I take this opportunity to express my indebtedness to Dr. L. Mansinha for his guidance and encouragement throughout the course of this research.

I would also like to thank John Brunet and Barry Price for devoting some of their time in discussing ideas involved with the instrumentation.

Finally I would like to express my appreciation to Dr. H.H. Schloessin for his constant interest and many helpful suggestions during my undergraduate career.

LIST OF FIGURES

1) INTRODUCTION

i) ACOUSTIC EMISSION

Acoustic Emission (A.E.) is the term applied to the spontaneously generated elastic wave, produced by the irreversible deformation of a material which is subjected to stress. For this reason acoustic emission is also referred to as stress wave emission (S.W.E.).

The phenomenon of acoustic emission was first scientifically investigated by Kaiser (1950). In his investigation, the noise emitted during the deformation of various metals, was recorded by electronic equipment capable of detecting very low amplitude signals. From this study it was found that: a) the predominant frequency of the acoustic emissions varied proportionally with the loading on the specimen, and b) the point of maximum frequency of emissions was the yield stress of the material. Subsequently Schofield (1958) verified the existence of these acoustic emissions and observed two distinct types: a large, erratic, low frequency named "Burst type" (detected as decaying sinusoids) and a lower level steady, high-frequency named "Continuous type" (resembling white noise) (see fig. 1).

Fig. 1. Continuous and Burst Type signals

(after T.Licht 1979)

The processes which generate acoustic emission signals as well as their characteristic type of emitted signal are given in table 1 compiled by T. Licht (1979). These processes are nondestructive in nature, and not visible to the bare eye. As a result they may only be detected by remote sensors, which are positioned on the surface of the material to be tested. By comparing the arrival times of the elastic wave at several sensors, the localization of the source is possible (Rindorf 1981).

TABLE 1

POSSIBLE SOURCES OF ACOUSTIC EMISSION SIGNALS AND TYPES OF SIGNALS EMITTED T. LICHT (1979)

SOURCE	TYPE OF SIGNAL
i) Dislocation movements	CONTINUOUS
ii) Phase transformations	BURST (Single event)
iii) Friction mechanisms	?
iv) Crack formation and extension	BURST (Multiple events)

In contrast to the above mentioned nondestructive processes which generate acoustic emission signals of relatively low amplitude, the process of fracture is both a visible and destructive phenomenon and emits a large amplitude signal at the time of failure. Since the accumulation of one or more nondestructive processes in both time and space result in failure, monitoring the acoustic emission activity in structures has proven to be successful in giving warning of incipient failure. As a result, in the last 20 years, acoustic emission has gained increased recognition in the field of nondestructive testing (NDT), as well as in monitoring the structural integrity of bridges, aircrafts, pipelines and vessels, under stress.

ii) APPLICATION OF THE ACOUSTIC EMISSION METHOD IN EARTHAKE MODEL STUDIES

It is widely believed by geophysicists that earthquakes are caused by the brittle fracture of the earth's crust. The seismicity in a given crustal volume is expected to be a function of the state of stress and the resistance to faulting of that volume.

If the preparatory process of an earthquake involves changes in the state of stress, the local seismicity should reflect these changes and thus provide information on the preparatory process.

There have been many descriptions of premonitory patterns of seismicity established by the analysis of earthquake catalogues. The three basic patterns are: quiescence, migration of epicentres and activation (Keilis-Borok, 1980). These patterns do exist but their reliability as precursors is not yet established.

The precursory patterns mentioned above, are also observed in laboratory studies of elastic shocks emitted during the deformation of brittle rock (Mogi 1962a,b; Scholz 1968a,b,c,d). In these investigations the acoustic emission method is employed to monitor the elastic waves which correspond to small amplitude cracking events (microfractures), that precede total failure in rock samples under compressive stress (Mogi 1962b). It is generally found that microfractures initially occur at random throughout the sample, but prior to fracture they cluster about the ultimate fault plane (Scholz 1968b).

The interpretation and scaling of these experiments is quite difficult due to the lack of control over the fracture's dimensions, as well as the inability in determining the true mechanism which generated the acoustic emission signals observed in shear deformation.

iii) PURPOSE OF THIS STUDY:

Savage and Mansinha (1963) were the first to initiate and propagate a tensile fracture, using local concentration of thermal stresses, on a sheet of glass. The elastic wave (A.E.) radiated by the sudden extension of their fracture was employed as an elastodynamic source in that study of seismic radiation fields.

The thermal stress method is applied in this investigation to initiate, propagate and bend the path of a tensile fracture on a sheet of glass. Window pane glass is used for modelling material due to it's low cost, availability, isotropy and brittle behaviour.

It is the brittle nature of glass that makes it highly susceptible to fracture by the propagation of cracks (Van Vlak 1973). This process involves the stages of crack formation and extension, which emit their characteristic acoustic emission signals.

The acoustic emissions generated in this investigation are detected using piezoelectric transducers located on the surface of the glass sheet. The signals are in turn amplified, filtered and digitally stored in the memory of a digital oscilloscope for subsequent analysis.

The scope of this investigation is to study the acoustic emission pattern precursory to three large amplitude events, namely, fracture initiation, bilateral extension, and bending of the propagation path. The variation in amplitude and frequency of the acoustic emissions precursory to these large amplitude events, must be a function of the rate of crack formation and extension as well as being dependent on the length of the fracture and the state of stress at the crack tip. This simple two dimensional study of precursory acoustic emission patterns aims to model the dynamic behaviour of faults prior to rupture. Theoretical

studies of precursory behaviours (Dmowska & Li (1981), Kostrov & Das (1981) have proposed the presence of "asperities", mechanically stronger regions separating cracked regions, within the fault plane. According to these models the earthquake is caused by the fracturing of the asperity and the joining of the two cracked regions.

This hypothesis is well documented in this model by the mechanisms of crack formation and extension which occur in the "fracture-process zone" prior to fracture (Irwin 1960). We expect that precursory acoustic emission patterns exhibit similar characteristics to premonitory patterns of seismicity.

From the point of view that elastic shocks emitted prior to the formation of a tensile fracture in glass correspond to minor earthquakes, this experiment may be regarded to be a model study of earthquake sequences prior to a large earthquake.

It is to be remembered that evidence of purely extensional dislocation is rare for earthquakes. However it has been suggested (AKI) that sudden faulting may be the result rather than the cause of many earthquakes.

iv) PHYSICAL PROPERTIES OF GLASS:

Glass is a noncrystalline, amorphous, solid composed mainly of silica (SiO_2). The Young's modulus (Y) of glass had been theoretically determined by Griffith (1920) to be Y = 700 kbars. In practice, glass was found to break at stress values much less than it's theoretical tensile strength. It was in turn shown by Griffith that this discrepancy exists due to the presence of prexisting flaws in the body of the glass.

The quantity by which the tensile strength will be reduced due to the presence of a flaw, depends on the dimensions of the flaw and was calculated by Inglis (1913). This quantity is called the "stress concentration factor" and it represents the amount by which the local stresses will increase due to the appearance of a flaw. These stresses will concentrate at the tip of the flaw in a manner shown in fig. 2. For this reason a tensile stress of 300 bars has been estimated to be sufficient in causing fracture along the plane of 2 cm long "prexisting" scratch on a glass plate (Savage & Mansinha 1963; Mohanty 1969).

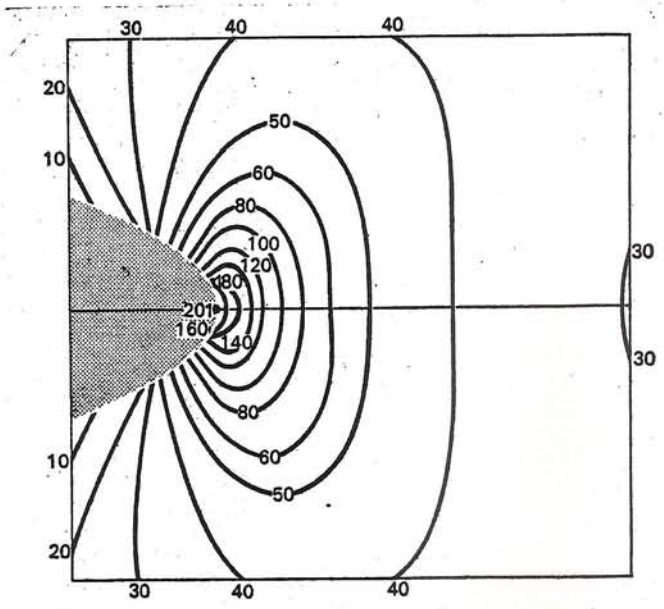

Figure 2. Stress system close to the tip of an elliptical crack. This is a map of the stress concentrations for stresses at *right-angles* to the plane of the crack, that is, parallel to the applied load. The shaded area represents the crack tip – that is, empty space. The curved lines are contours of equal stress concentration. The figures indicate the number of times by which the local stress is increased as compared with the mean stress remote from the crack. The maximum concentration of stress is about 200. The actual values of the stress concentration will, of course, vary with the length of the crack but the relative proportions remain constant.

(after J.Cook 1974)

Glass exhibits elastic behaviour up to 1.5% strain and being a brittle solid, fracture will occur by the spreading of cracks. Griffith (1920) stated that the general condition of rupture is the attainment of a specific tensile stress at the tip of a crack. Irwin (1960) and Marsh (1969a,b) have shown a zone of plasticity to exist at the crack tip. It is within this "fracture-process" zone that small separations form and grow, releasing strain energy. Irwin (1957) postulated that the release of strain energy is directly related to the tensile stress at the tip of the crack. A certain portion of this strain energy is dissipated in the release of elastic waves which are detected in this experiment. The continuous monitoring of elastic waves radiated for different stress distributions at the crack tip may give some insight to the release of strain energy as a function of applied stress.

v) PHYSICAL PROPERTIES OF THE DETECTORS (PIEZOELECTRIC TRANSDUCERS):

Piezoelectrics are dielectric materials with assymetric structures such that their centres of positive and negative charges do not coincide. Thus the polarity is sensitive to pressures which change the dipole distance and the polarization (Van Vlack 1973). When this dipole distance is altered, the dipole moment changes such as to produce: a) electron flow from one electrode to the other, if the two are connected, or, b) voltage change between the two electrodes, if the two are not connected (fig.3).

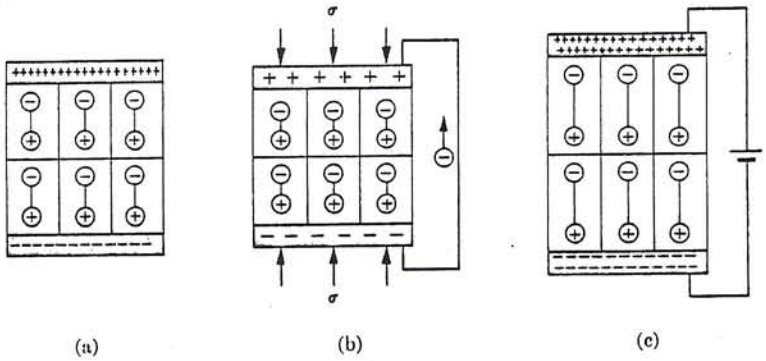

Fig. 3 : Piezoelectricity. (a) The dipoles within the material produce a charge difference between the two ends. (b) Pressure shortens the dipoles, and therefore reduces the charge density on the two electrodes (or introduces a voltage difference if the two ends are not shorted). (c) An external voltage alters the dipole lengths.

(after L.Van Vlak 1973)

Transducers are materials or devices which convert one form of energy to another. In this sense piezoelectric materials perform the reversible phenomenon of transduction of mechanical vibration to an electrical signal and vice versa. This property is utilized in seismic modelling (Oliver et al 1954) where piezoelectric crystals are employed both as a source as well as a receiver.

In this particular study ceramic piezoelectrics of the barium-titanium ($BaTiO_3$) family were used both as a source and detectors. These bimorph, plate shaped transducers posses a high directional sensitivity along a plane perpendicular to the plate (fig. 4).

Figure 4
Piezoelectric crystal.

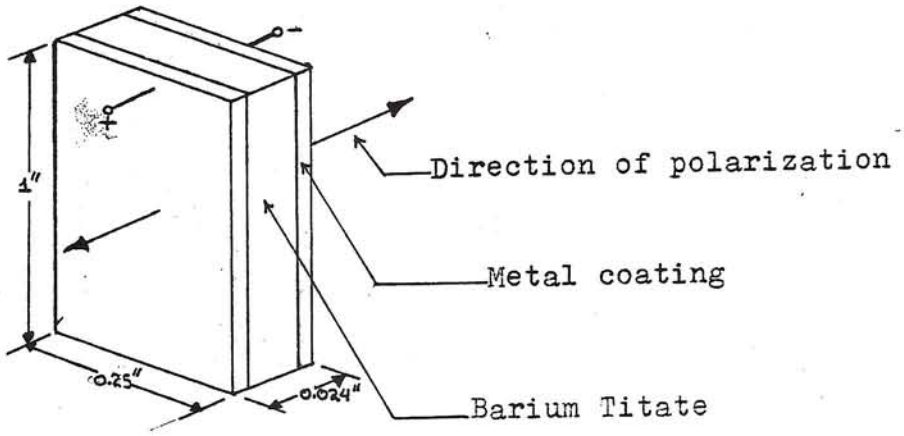

The small size and great stiffness (sensitivity) of these ceramic crystals allows for their application in acoustic emission studies (Egle and Tatro 1966), as detecting elements of stress waves that propagate on the surface of the strained material.

vi) ELASTIC WAVE PROPAGATION BEHAVIOURS IN SOLID MEDIA

This experiment primarily involves the detection of elastic stress waves which propagate on the surface of a glass plate. Some basic propagation behaviours of these waves shall be discussed in this section in order to give insight to the geometrical design of this two-dimensional model.

It is generally known that two basic forms of elastic waves are emitted from an acoustic emission source in an infinite medium. Each form has a characteristic velocity of propagation which depends on the density and elastic constants of the solid medium. These two forms are:

a) longitudinal or p-waves, and b) transverse or s-waves (Dobrin 1976). With reference to figure 5 we note the particle motion associated with a) longitudinal waves, to be parallel to the wave propagation direction, and, b) transverse waves, to be perpendicular to the wave propagation direction. The radiation pattern of these two types of waves from an acoustic emission source is shown in figure 6.

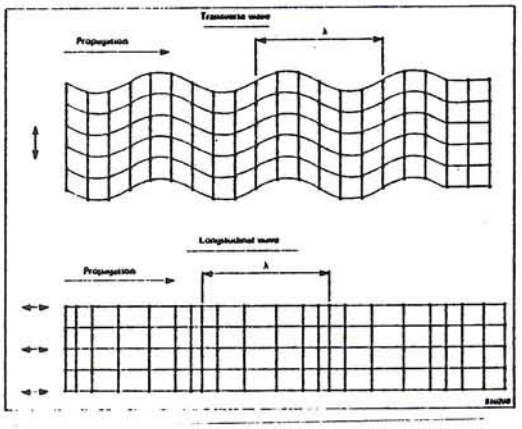

Figure 5 :The two basic wave modes in a solid. (after J. Rindorf 1981)

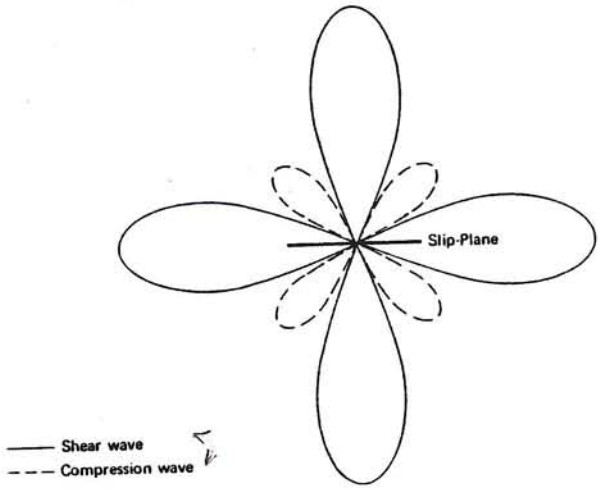

Figure 6 :Radiation pattern from a source. (after T.Licht 1979)

Upon the introduction of a surface the longitudinal and transverse waves will combine in a region close to the surface to produce a surface wave called Rayleigh wave. The particle motion of a Rayleigh wave is

Figure 8 : The two basic wave modes in a plate.
(after J.Rindorf 1981)

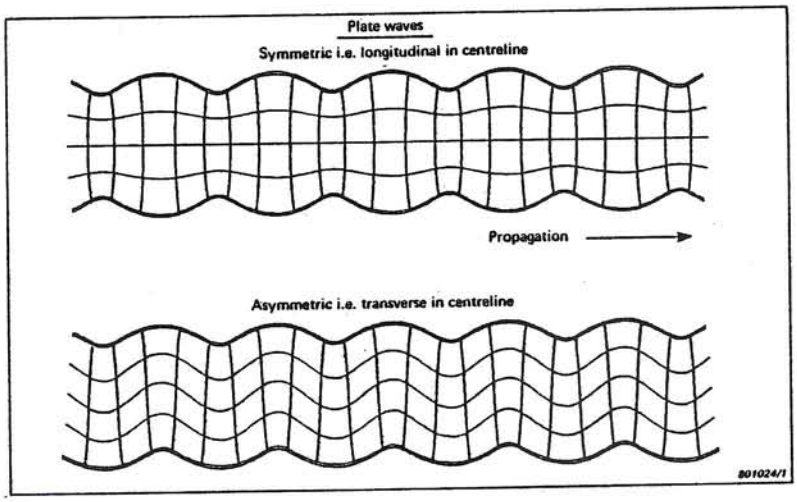

The two-dimensional modelling theory of Oliver et al (1954) established an analogy between the symmetric plate wave in a two-dimensional model and the longitudinal wave in a three dimensional model. The basic requirement for the fulfillment of two-dimensional modelling is that the thickness of the plate be small in comparison to the wavelengths observed, so that dispersion is minimized.

A further consideration in two-dimensional modelling is the source-detector distance necessary to satisfy the far-field approximation. Savage and Mansinha (1963) showed that a source-detector distance of 4 wavelengths sufficiently approximates the far-field, and provides excellent agreement with theory. In view of the above considerations we may proceed in the design of this two-dimensional model.

2) DESIGN OF TWO DIMENSIONAL MODELS

The primary steps in the design of a model are: a) the accurate representation of the situation to be modelled, and b) the appropriate scaling of the model to the real situation.

In this particular experiment an attempt is made to model the microearthquake activity which is precursory to a large amplitude earthquake. This precursory activity has been associated with the process of crack formation surrounding an asperity in the fault plane (Dmowska and Li 1981). The large amplitude earthquake is associated with the fracturing of the asperity and the joining of the pre-existing cracks.

As it was stated earlier, the phenomenon of brittle fracture in glass is governed by the processes of crack formation and extension. In the case of a tensile fracture these are the only processes which precede fracture. It should be noted that fracture in glass is not entirely a surface phenomenon and the governing processes take place throughout the thickness of the plate, in this case throughout the plane of a preinscribed scratch. The similarity in the processes involved leads us to believe that the process of crack formation and extension prior to brittle fracture in glass is a fairly accurate representation of the preparatory process of an earthquake. The lack of an exact similitude however exists if we consider the generally accepted theory that most earthquakes are due to shear fracture. The justification for using a fracture model in a plate, in order to simulate a fracture in a three dimensional model, has been satisfactorily defended by Savage and Mansinha (1963).

In this investigation tensile fractures are employed due to the relative ease with which they are initiated and propagated. The use of thermal stress in the construction of tensile fractures in glass allows the experimenter great control over the dimensions of the desired fracture and as a result the subsequent scaling of the model is possible. Another advantage in using tensile fractures is the capability of identifying the stages of crack formation and extension by the analysis of their characteristic acoustic emission signals. The introduction of friction due to shear stress would tend to complicate the identification of the processes involved, since there is no characteristic acoustic emission signal associated with that process (see table 1).

i) TECHNIQUES FOR FRACTURE FORMATION AND ASSOCIATED STRESS FIELD DESCRIPTION

The concept of producing tensile fractures in glass plates by means of thermal stress has been used successfully in the past by many investigators (Savage and Mansinha 1963, Mohanty 1969). The principles involved in initiating and propagating tensile fractures are: i) the general condition of rupture stated by Griffith (1920), and: ii) the assumption that the fracture will propagate in the direction of maximum tangential tensile stress (Mansinha 1964).

A small gas torch provides a low temperature flame which is applied on the horizontal surface of the glass. The diameter of the flame is approximately 1 cm and the temperature distribution is radially symmetric about the centre of this heated zone. This thermal gradient produces differential expansion about the centre of heat application and as a result radial and tangential (hoop) stresses are developed in the glass

plate. The compressive radial stresses increase towards the centre of the heated zone while the tensile hoop stresses reach a maximum at about 3-4 cm from this centre as observed during experimental tests. Local concentration of thermal stresses about an existing flaw will lead to the superposition of the above stress components. In general the tensile hoop stresses must be concentrated at the centre of the flaw to initiate a tensile fracture, while the compressive radial stresses must be concentrated at the tip of the propagating fracture in order to control the velocity and direction of propagation as well as the dimensions of the propagating fracture.

To initiate a tensile fracture, a 2 cm long scratch is inscribed on the surface of the glass using a sharp metal scribe and relatively light scoring pressure. The centre of the flame is then applied 2.5 cm from one end of the scratch at A, (see fig. 9a) for approximately 30 seconds. Then the centre of the flame is applied the same distance away from the other end of the preinscribed scratch, at B, for another 30 seconds. This procedure is repeated for approximately 4 minutes at which time a fracture will suddenly form.

The initiation of this fracture is followed by the sudden extension of both ends towards the two heated zones A and B. Upon removal of the heat source, follwing this extension, both tips of the fracture are observed to stop approximately 1.5 cm from the heated zone centre. This stopping is due to the high compressive radial stress encountered by the fracture tip on approach to the centre of the heated zones. The resultant 4 cm long, symmetrical, fracture is called "bilateral" and is constructed in model I.

Figure 9a : MODEL I , BILATERAL FRACTURE

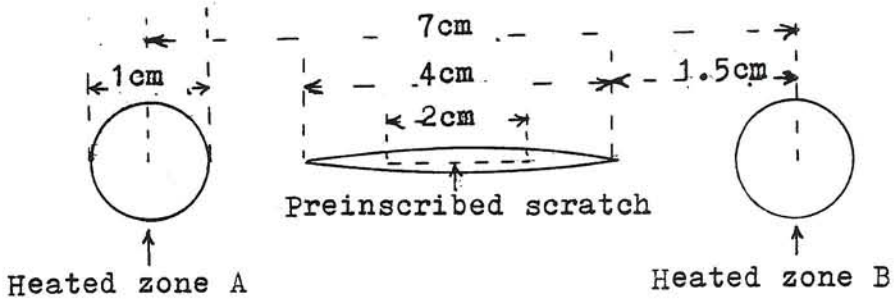

In the subsequent two models a bilateral fracture is initiated by the procedure described above and then is propagated in one direction only. In order to propagate this fracture the hoop stresses at the chosen stationary tip must be larger than the compressive stresses at the propagating tip.

In model II, upon initiation of a bilateral fracture, choosing A to be the stationary side (see fig 9b), the flame is applied at C, 5 cm from B, for approximately 45 seconds. Then the flame is applied at B for approximately 15 seconds and in turn at A for 30 seconds. The fracture is observed to propagate very slowly through the heated zone at B and then suddenly extend towards C, this being the direction of maximum hoop stresses. The duration of propagation is roughly 15 seconds and the resulting unilateral fracture is 8 cm long. This unilateral fracture is constructed in model II and is allowed to propagate through a region (B) of compressive stress.

Figure 9b : MODEL II, UNILATERAL FRACTURE

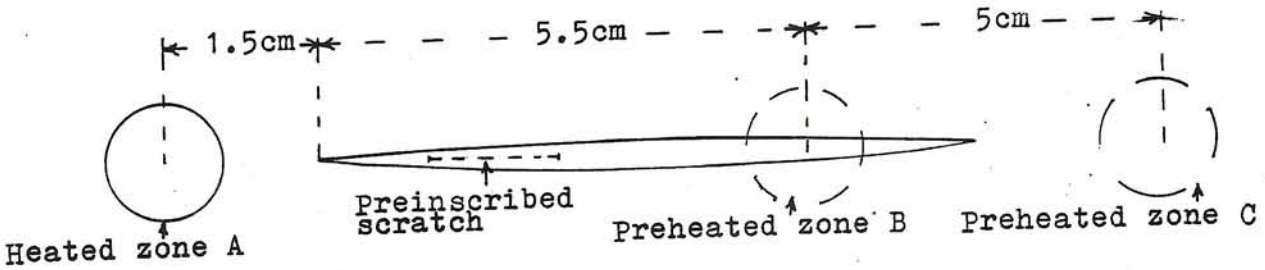

In model III (see fig 9C) a shorter unilateral fracture is propagated towards the center of a high radial compressive stress zone. In this case the fracture does not propagate through this zone due to the intensity of radial compressive stress acting at the propagating tip. Initially a bilateral fracture such as that of model I is formed and upon formation the flame is applied at A, the chosen stationary tip, for 30 seconds. The hoop stresses at the stationary tip build up and exceed the radial compressive stresses at the other tip causing the unilateral propagation towards B, for roughly 1 cm. The fracture is observed to stop propagating at this point and is followed by a sudden bending of its path at a 45° angle on either side of the heated zone at B. The duration of this fracture propagation and bending is roughly 40 seconds. We note that the heated zone B stops the propagation of the fracture at a point where the radial compressive stresses due to the heated zone at B exceed the hoop stresses due to the heating at A. The sudden bending of the path occurs due to the superposition of hoop

stresses, tangential to the circular zone of radial compression at B.

Figure 9c: MODEL III, BENDING FRACTURE

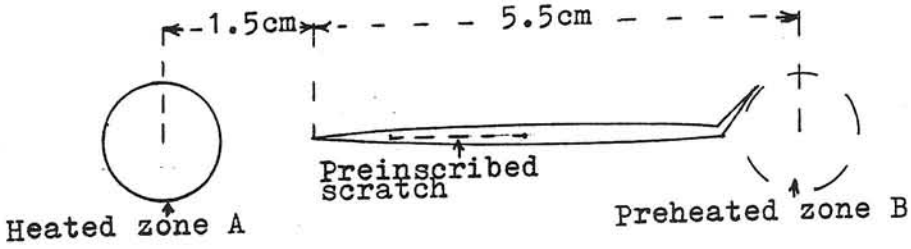

Care was taken in all experiments to maintain the dimensions and scoring pressure of the inscribed scratch constant as well as maintaining the diameter of the flame constant. These are the important parameters in determining the dimensions of the original bilateral fractures. During experimental tests it was found that an 80% dependability for reproducing any of the three fracture types is attained with the above described techniques.

The next important consideration in the design of this model is the appropriate scaling of the model employing the principles of two-dimensional modelling theory discussed in the previous chapter. Since the dimensions and the location of the fractures involved in the three models are controlled by the experimenter, the orientation of the detectors must be determined to ensure maximum p-wave sensitivity from the emitted acoustic emissions. The actual location of the detectors and the size of the glass plate models will be subsequently determined in accordance to the two-dimensional modelling theory.

ii) GEOMETRICAL DESIGN OF MODEL

Throughout this study reference to the coordinates of a position on the glass surface will be made using an azimuth angle and a distance away from the centre of the preinscribed scratch. For this purpose it is necessary that the reader becomes familiar to this notation described in figure 10.

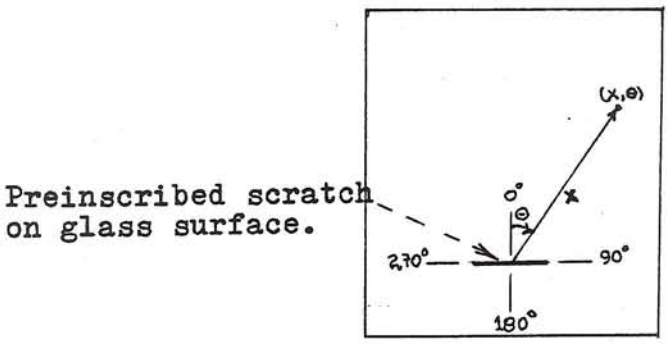

Figure 10: Coordinate system of 2-D models.

First we must consider the radiation pattern of acoustic emission events which occur during the tensile fracture process in glass plates. Studies of the radiation pattern from: a) the initiation of a tensile fracture (Mohanty 1969), and b) the extension of a tensile fracture (Savage and Mansinha 1963), both exhibit similar characteristics. In general a p-wave maximum exists along the direction of applied tension, $\theta = 0^{\circ}$ and $\theta = 180^{\circ}$, and a minimum at right angles to it, $\theta = 90^{\circ}$ and $\theta = 270^{\circ}$. The direction of maximum s-wave direction is along the $\theta = 45^{\circ}$ azimuth.

In view of the qualitative agreement for the radiation pattern from two different generating processes we shall assume all events occurring within the preinscribed scratch plane to exhibit the above radiation pattern.

The detection and localization of the acoustic emission events requires maximum sensitivity of p-waves. With reference to figure 11 we proceed to describe the appropriate geometrical positioning of the detectors with respect to the source.

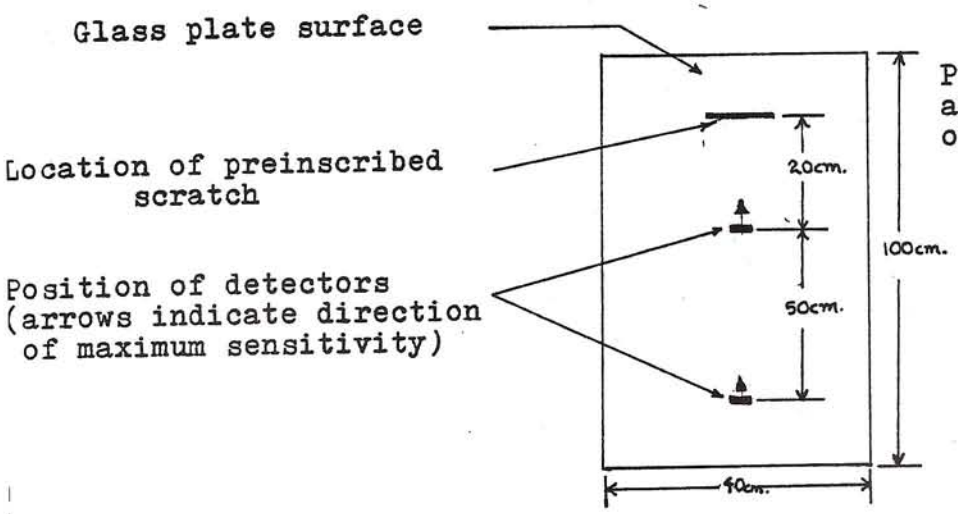

Figure 11: Position of detecting array for the recording of acoustic emissions.

For the purpose of initiating the digital recording of the acoustic emission activity at the onset of deformation, a trigger piezoelectric crystal is positioned at the $\Theta = 180^{\circ}$ azimuth, within 3 cm from the source. The orientation of this crystal is such as to ensure maximum p-wave sensitivity.

Two other piezoelectric crystals required to detect the acoustic emission activity in the course of the experiments are positioned along the $\Theta = 0^{\circ}$ azimuth, both oriented for maximum sensitivity to p-waves. The first detector is fixed at 20 cm from the source to approximate the far-field. The second detector is positioned at variable distances from the source (40, 50, 60, 70, 80 cm) to measure the p-wave velocity of glass. This same detector positioned at 70 cm from the source also

serves the purpose of localizing the acoustic emission events in all experiments. For the purpose of localizing the source of the acoustic emissions along the line which contains the preinscribed scratch, two detectors are required. The difference in distance travelled by a wave to the two detectors can be calculated from the measured time difference. A geometrical approach to the problem of localizing events occurring along a line, using two detectors located along a perpendicular line, is outlined in appendix I. The geometrical arrangement of the fracture and the detectors on the surface of glass requires a rectangular sheet of glass dimensions 100 x 40 cm. The thickness of the glass plates must be small compared to the wavelength of the acoustic emissions. Savage and Mansinha (1963) estimated a wavelength of 5 cm at 100 khz and used a plate thickness of 0.3 cm. This same plate thickness is used in these models.

It is worth noting that the geometrical design of these models provides ultimate sensitivity to p-wave detection as well as satisfying the basic principles of two-dimensional modelling.

iii) INSTRUMENTATION

Previous studies of acoustic emission signals in glass plates indicate the frequency of signals to be in the 100 khz range (Savage and Mansinha 1963). The instrumentation involved in this study is designed to detect signals in the frequency range of 1 khz to 150 khz.

Three bimorph plates (0.25"W x 1"L x 0.024" T) serve as the detecting crystals. Each plate is mounted to a wood rod in a manner shown in figure 12. The resulting detector is then allowed to rest perpendicular on the glass surface, under the influence of its own weight. A drop of

liquid silicone is placed between the crystal and the glass surface to improve the coupling. Special care is taken in using crystals and wood rods of the same size, in all the detectors to ensure similar sensitivity and coupling.

Figure 12:
Detector design
(Direction of maximum sensitivity is indicated by arrow)

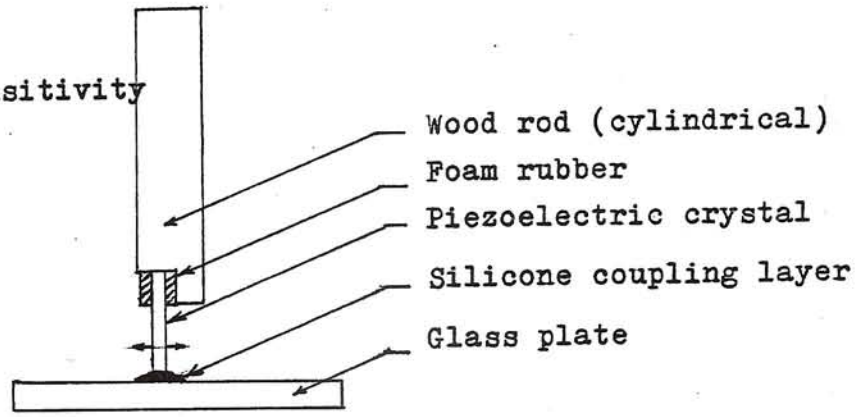

Shielded cables are used to transmit the electric signal from the detectors to the amplifiers. The length of the cable was kept at a minimum (15-20 cm) to reduce electromagnetic noise present in the signal. A detector design which has efficiently reduced noise in the signals was constructed upon completion of this study and shall be discussed in appendix II.

Two detectors served the purpose of continuously monitoring the acoustic emission activity during the course of each experiment, and one detector was used as a trigger, initiating the recording of any activity at the onset of deformation.

Figure 13 : Electronic Instrumentation Design

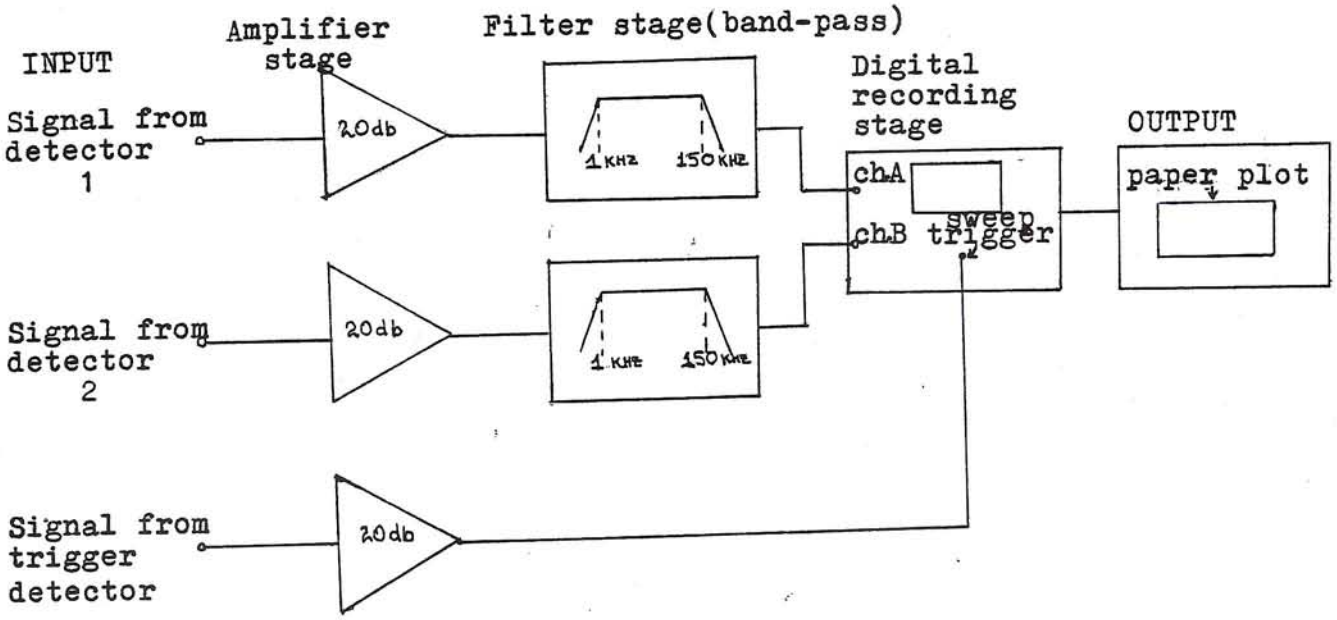

With reference to figure 13 the electronic instrumentation is described. The signal from each of the two detectors is amplified using the two vertical amplifiers of a Tectronix 555 cathode ray oscilloscope. A gain of 20 db is shown to be sufficient in bringing the low amplitude events above the existing noise level. The frequency response of the amplifiers is flat up to 150 khz.

The amplified signals are in turn filtered using two Krohn-Hite 315A band-pass filters. A low cut-off frequency of 1 khz and a high cut-off frequency of 150 khz proved efficient in eliminating most of the noise. The attenuation slope at the cut-off frequencies is 12 db/ octave and the filters exhibit unity gain within this frequency range.

Next the amplified and filtered signals are inputs to a two channel digital oscilloscope (Nicolet model #2090). The two signals are sampled and digitized at intervals dependent on the selected sweep rate, and are subsequently stored in the buffer memory upon completion of the triggered sweep. The buffer memory for each channel of this digital oscilloscope has a storage capacity of 2048 points per sweep, but it is also possible to trigger two consecutive sweeps with a storage capacity of 1024 points per sweep. Once the data is stored in the memory it is possible to expand the horizontal or vertical part of any portion of data by a factor ranging from two up to sixty-four. This expansion is digitally accomplished and the coordinates (time, voltage) of any point may be read directly on the screen. A permanent record of any desired portion of results is obtained by transferring of the data from the buffer memory to an X-Y plotter. Initiation of a sweep on the digital oscilloscope is performed by means of comparing the voltage level of an incoming signal from the trigger detector to a preselected trigger threshold on the oscilloscope.

Since the output voltage of the piezoelectric crystal, arising from an acoustic emission event, is too low to be compared to the trigger threshold, an operational amplifier circuit was constructed to boost the signal from the trigger detector by 20 db.

3) EXPERIMENTATION

i) EXPERIMENTAL PROCEDURES

The sheet of glass to be used in each experiment is cut to size (100 X 40 cm) and is supported horizontally by rubber foam such that bending stresses are minimized.

Next the location of the inscribed scratch and the relative positions of the detectors is established as shown in figure 11. A drop of silicone is placed on the glass surface at the location of each detector which is in turn allowed to rest freely on the silicone layer.

As it will be discussed in a later section the insufficient storage capacity of the Nicolet digital oscilloscope allowed the localization of only the first acoustic emission in each model. All subsequent acoustic emission activity was sampled at a frequency much less than their Nyquest and a result they appear as single spikes on our records.

Once the appropriate sampling frequency for the localization of the first acoustic emission is chosen, the instrumentation is set on trigger standby and the procedure for forming any one of the three desired fractures is followed.

Upon the occurrence of the first acoustic emission event to overcome the trigger threshold, a sweep is initiated and stored. This sweep contains the p-wave arrival at two detectors which is to be used in locating this first event. Immediately following this a second sweep is automatically initiated and the sampling frequency is manually

adjusted to a value which allows the sampling of all subsequent acoustic emissions in the model. This manual selection is performed in a matter of a few seconds and as a result the possibility of missed events in this time interval is minimal.

ii) EXPERIMENTAL TESTS AND OBSERVATIONS

Prior to obtaining results for analysis it is necessary to perform some experimental tests and observations to ensure the proper functioning of the instrumentation and good quality of results obtained.

a) Determination of velocity

This first test is performed to obtain an accurate value for the longitudinal wave velocity of the glass plates used in this study. This result will later on be used in the localization of events and is therefore essential. By comparing this result with ones obtained from previous studies, we are in a way testing the accuracy and performance of the electronic instrumentation.

The "fixed source and variable detector spacing" method is used and the experimental set-up is described with reference to figure 14.

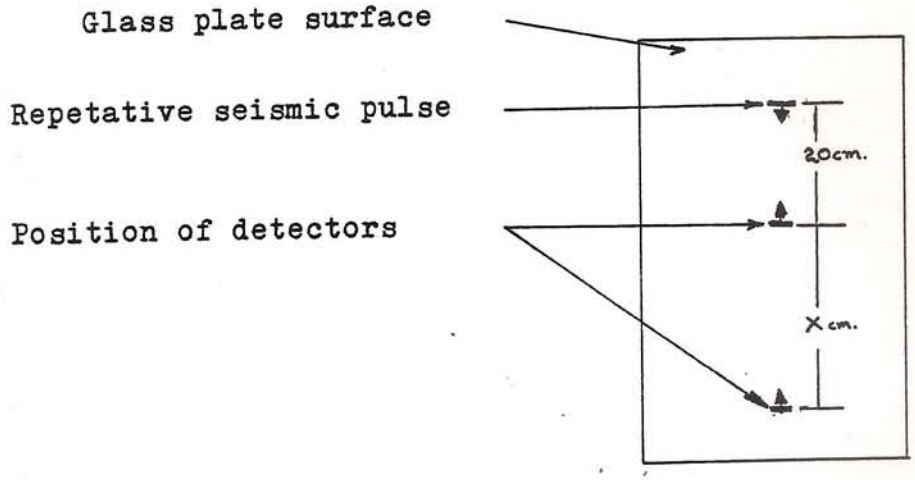

Figure 14 : Experimental set-up for measuring the p-wave velocity of glass. Arrows indicate direction of maximum p-wave sensitivit of the detector

A sheet of glass (100 X 40 X 0.3 cm) is supported horizontally with rubber foam. A piezoelectric crystal is utilized for the purpose of transmitting a seismic signal with one of the designed detectors. By applying a voltage pulse to this piezoelectric crystal, positioned as shown in figure 14, a seismic signal is emitted in the glass with maximum p-wave radiation in the $\theta = 0^{\circ}$ and $\theta = 180^{\circ}$ azimuths. In order to provide a fair representation of a burst type acoustic emission signal, the amplitude of the emitted repetitive pulse is kept at a minimum (millivolt range) and the frequency at a maximum (roughly 100 khz).

A detector positioned 20 cm from the transmitter along the $\theta = 0^{\circ}$ azimuth and oriented for maximum p-wave sensitivity, is allowed to rest freely on the glass surface. Similarily a second detector is positioned in line with the first one at various distances from the source (40, 50, 60, 70 cm). A drop of liquid silicone is placed between each of the three crystals and the glass. The signals from the two detectors are amplified and filtered before being displayed on the digital oscilloscope whose sweep rate is matched with that of the emitted pulse.

The difference in arrival time of the emitted pulse between the two detectors is measured accurately on the digital oscilloscope, for four different detector spacings. The ratio of the distance between the two detectors to the measured difference in arrival times, for the various spacings, gives the value of the longitudinal (p-wave) velocity of glass. This test was repeated several times, on many different sheets of glass and with the array placed at various orientations on the

surface of the glass always sensitive to the p-wave radiation. The value of the p-wave velocity was found to remain constant at V_p = 5416.66 ± 20 m/sec. The consistancy of this value indicates high confidence in these measurements and also the isotropy inherent in glass. The errors involved in measuring the above value are due to errors in measuring distances ± 1 mm, minimized due to the thin plates used as detectors, and errors in picking first arrivals, ± 0.25 μsec, minimized due to the high sampling rate 1 μsec/point and allowable expansion of the desired portion of the signal, four times.

When the above value of p-wave velocity is compared to those experimentally obtained by several investigators, it is found to be in excellent agreement within the calculated error margin.

b) Observations of acoustic emission signals

Next the characteristic amplitudes and waveforms of the acoustic emissions occurring in the three models are observed, for the purpose of selecting the appropriate sampling rate and trigger level to be used in the recording of events. The experimental methods and fracture formation techniques discussed earlier are employed to observe the acoustic emissions which occur in each of the three models.

First by manually adjusting the gain of the amplifiers and noting the resulting amplitude of the emitted signals, a gain of 20 db is decided to be sufficient in boosting the signal of the low amplitude events above the existing continuous noise level. Next the trigger threshold of the Nicolett oscilloscope is adjusted to be above this continuous noise level and therefore be overcome only upon the occurrence

of an acoustic emission of the burst type nature.

The experiment of initiating a fracture was repeated to test this trigger threshold and it was observed that the presence of random electromagnetic noise activates the trigger threshold. When the level of this threshold is brought above the random noise level, the possibility of small amplitude events not triggering the electronic instrumentation exist but cannot be avoided.

By recording and analysing some acoustic emissions the characteristic burst-type waveform is observed, as seen on figure 15. This event represents a single impulse of energy which is detected as a decaying sinusoid. The decay time of these sinusoids is found to range from 30 to 100 msecs and is amplitude dependent. In contrast, the decay time of the randomly occurring spikes of electromagnetic noise is much less (10-20 msec) and thus we may distinguish their presence in our records.

FIGURE 15 : CHARACTERISTIC WAVEFORM OF BURST-TYPE ACOUSTIC EMISSION SIGNAL

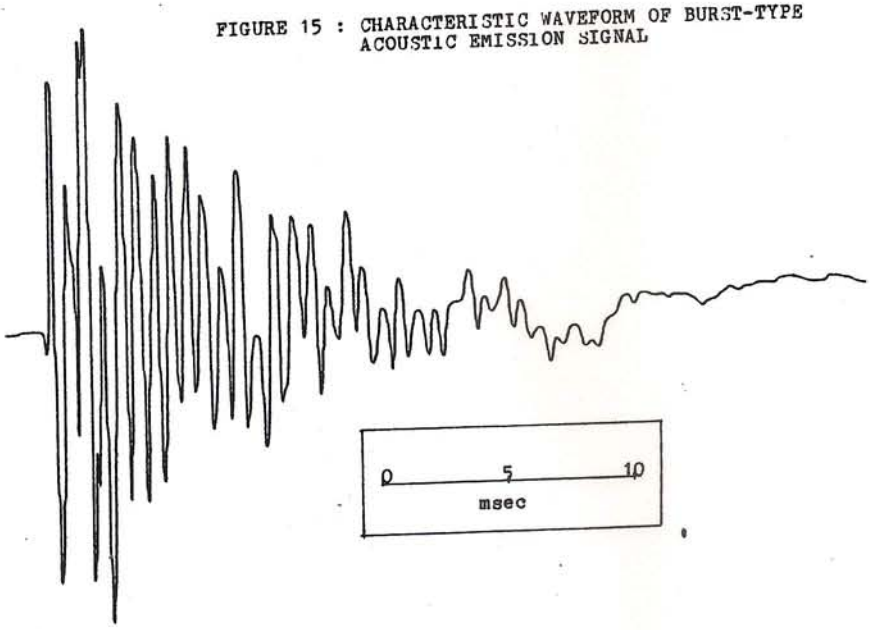

During several observations of the acoustic emission activity associated with each model, it was noted that several small amplitude acoustic emissions precede the formation of the desired fracture.

The localization of each event along the preinscribed scratch plane requires a sampling rate of 1 μsec/point to minimize errors in picking first arrivals. The storage capacity required for this sampling rate over a fracture propagation duration of roughly 40 seconds (model III) exceeds the storage capacity available in the nicolet digital oscilloscope (1024 points/sweep). As a result of this restriction and in view of the capability of the oscilloscope to sample and store two consecutive sweeps per channel, the localization of the first acoustic emission will take place upon triggering of the first sweep, with a sampling rate of 1 μsec/point. The subsequent sweep will be sampled at intervals ranging from 20 msec/point to 50 msec/point and thus be sufficiently long to sample all subsequently occurring events at least once.

In interpreting the obtained results it is important to consider that this choice of sweep rates may sample a single large amplitude event more than once, while completely missing a low amplitude event due to the decay time associated with these acoustic emissions.

c) Microscopic observations

The use of an optic microscope provides an accurate picture of the fracture plane induced in the sheets of glass from the various models. A magnification of 200 was used to reveal the following characteristics:

In Plate 1 the tip of a bilateral fracture is photographed under crossed nicols. The stress distribution in the region ahead of the fracture tip is observed and the light regions are believed to be the possible areas of plastic deformation or fracture process zones.

Plate 2 reveals the bending angle of the fracture propagation observed in model III. This bending of approximately 45° takes place upon approach of the fracture tip to the region of high compressive stress. The direction of bending coincides with the direction of maximum tangential tensile stress.

Plate 3 reveals the irregular nature of the fracture wall 2mm ahead of the visible crack tip. The appearance of unbroken regions (dark) separating cracked regions (light) indicates that these irregularities may be the cause of the crack formation and extension mechanisms which generate the observed acoustic emission signals. It is believed that these observations will aid the data interpretation process since the generating mechanisms of the acoustic emission signals are not visible to the naked eye.

PLATE 1: STRESS CONCENTRATION AT FRACTURE TIP.
TOTAL MAGNIFICATION 200X.

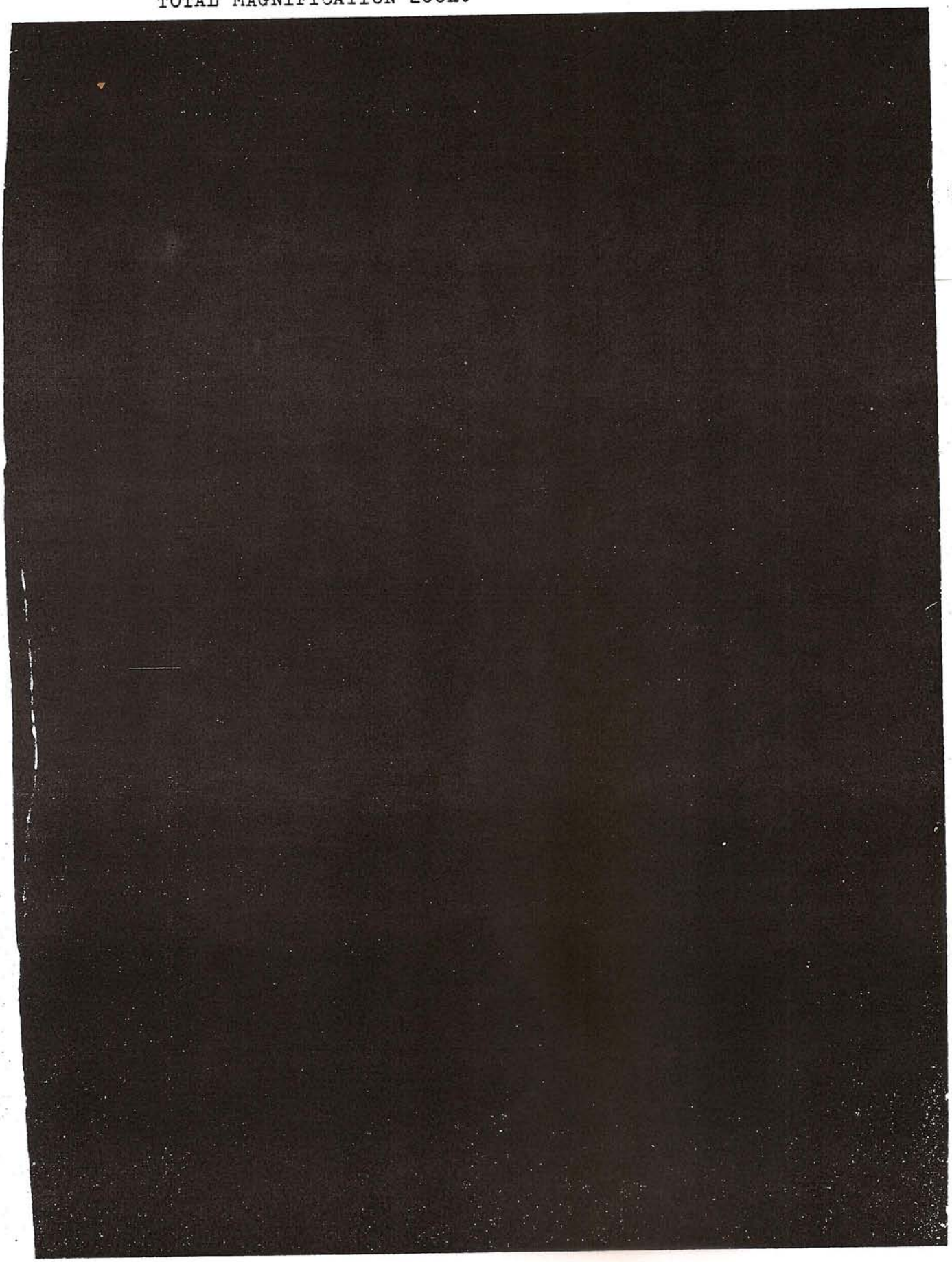

PLATE 2: BENDING OF FRACTURE PROPAGATION
TOTAL MAGNIFICATION 200X.

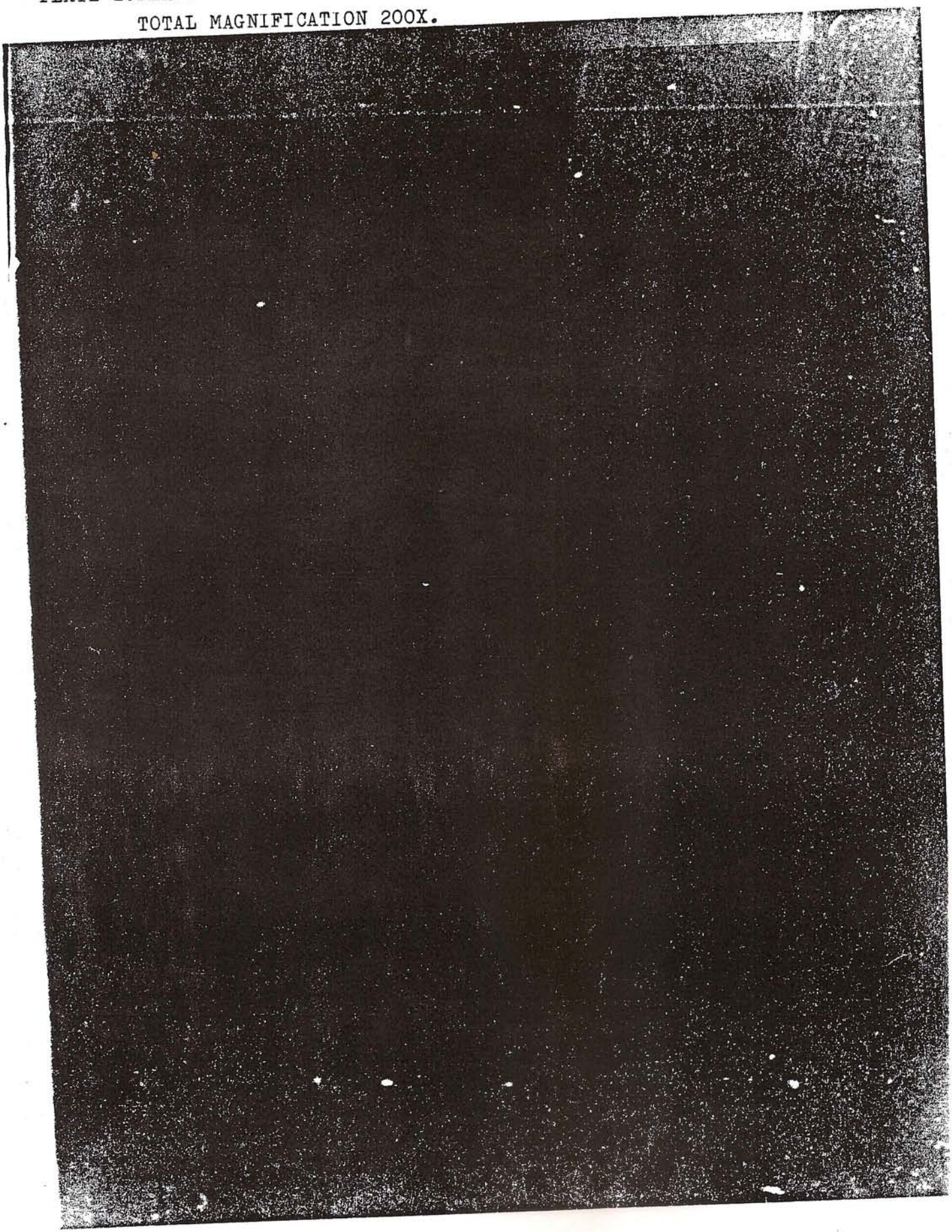

PLATE 3: FRACTURE WALL IRREGULARITIES
TOTAL MAGNIFICATION 200X.

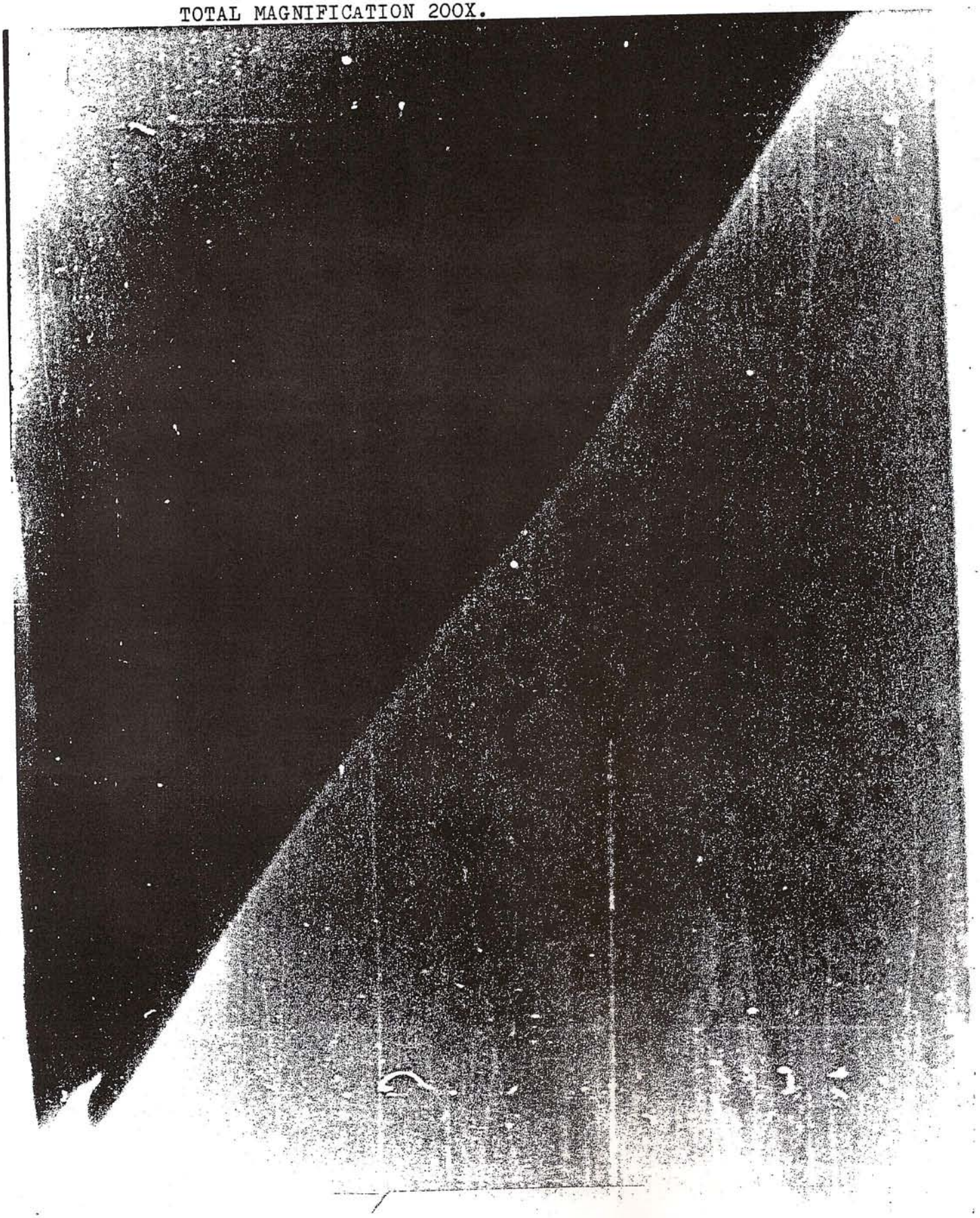

4) R E S U L T S

In this section some results of the acoustic emission activity associated with each of the three models are presented and interpreted. It is expected that the variation in the frequency and amplitude of the acoustic emissions is a function of the applied stress at the tip of the fracture. These results are chosen from a total of 10 to 15 controlled experiments involving each model, and they are quite representative of the overall observed acoustic emission patterns in each case.

a) Model I

The acoustic emission activity associated with the initiation of a 4 cm long bilateral fracture is monitored in this model. During the course of experimentation it is observed that a large amplitude acoustic emission event overcomes the trigger threshold and characterizes the formation of this bilateral fracture. No other events are detected prior to, or, following this burst type event which has a characteristic decay time of 100 msec (see fig. 16).

FIGURE 16 : ACOUSTIC EMISSION SIGNAL GENERATED BY A BILATERAL FRACTURE

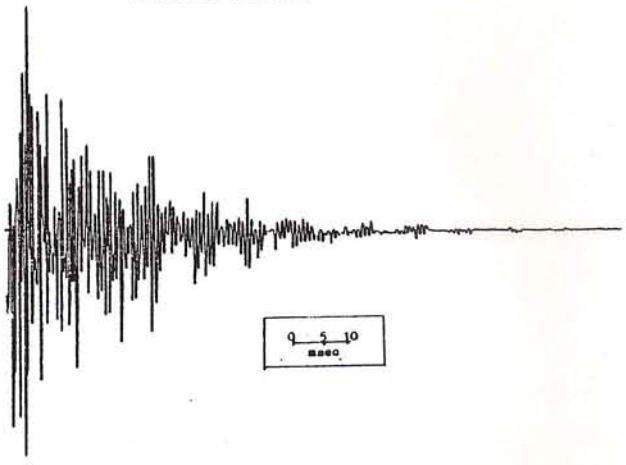

200 d/o

The localization of this acoustic emission shall provide some insight regarding the location of the deformation mechanism which generates this event. This deformation is expected to start at the center of the preinscribed scratch plane since this will be the location of maximum tensile stress, due to the superposition of the stress components from the two heated zones on either side of the scratch.

The experiment set-up shown in figure 11 shall be used to measure the difference in arrival time of the emitted p-wave at the two detectors positioned 50 cm apart. In appendix I the method for locating the source of this p-wave is described and the earlier measured value of p-wave velocity, V_p = 5416.66 m/sec, is used.

In locating the source of this first acoustic emission we must ensure that triggering of the sweep on the Nicolet oscilloscope occurs prior to the p-wave arrival at the two detectors. For this purpose a trigger detector is placed within 3 cm of the source. Thus the p-wave arrival at the closest detector will occur 15 msec following the triggering of the sweep. Any further delay in triggering due to a slow rise-time (slew-rate) of the operational amplifier used in the trigger circuit, must be avoided. In this trigger circuit a high slew rate, 10 V/μsec, operational amplifier is employed to minimize this problem.

The sampling rate used for the localization of this event is 1 μsec/point which allows an error of ±0.25 μsec in picking first arrivals. Distances are measured with an accuracy of ± 1 mm due to the thin

piezoelectric plates used as detectors. A typical example of the p-wave arrival at the two detectors for the first acoustic emission to overcome the trigger threshold in Model I is shown in figure 17.

FIGURE 17: P-WAVE ARRIVAL AT TWO DETECTORS SEPERATED BY 50cm.

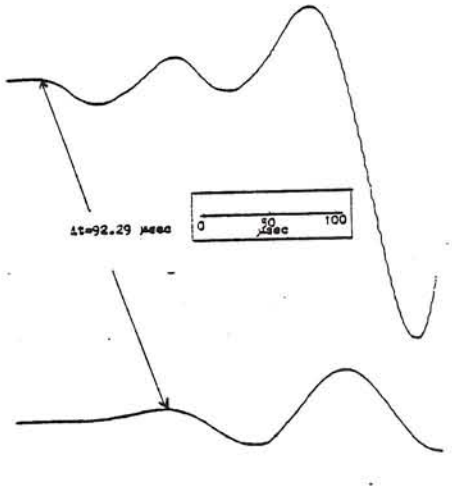

The difference in arrival times is measured to be 92.29 $\pm$ 0.25 μsec which locates the event 0.05 $\pm$ 0.01 cm away from the end of the pre-inscribed scratch. It should be noted that the method of locating events as outlined in appendix I, yields twin solutions symmetrical about the centre of the preinscribed scratch. The location of this event shows that deformation is initiated along the line containing the preinscribed scratch but not at the centre of the preinscribed scratch as expected. It is believed that the high trigger threshold level did not allow any small amplitude events to be recorded prior to the spontaneous opening of the bilateral fracture wall.

Since the trigger threshold level is set to be above the random electromagnetic noise level, to avoid false triggering, it is not possible at this point to detect the presence of any precursory acoustic emission activity in this model.

The localization of this first acoustic emission to overcome the trigger threshold is important in ensuring that deformation is initiated along the line containing the preinscribed scratch rather than anywhere else on the model surface.

b) Model II

The acoustic emission activity associated with the propagation of a unilateral fracture through a zone of compressive radial stress is analyzed in this section.

A bilateral fracture such as in model I is initiated and is in turn propagated unilaterally towards a zone of compressive radial stress. The velocity of propagation is observed to decrease on approach to, and through, this zone. A sudden extension is observed when the unilateral fracture has propagated through the zone of compressive radial stress and encounters a zone of tensile hoop stresses.

The resulting unilateral fracture is roughly 8 cm long and the duration of this propagation is roughly 15 seconds. Figures 18,19,20 show the acoustic emission activity associated with this propagation. The sampling rate of 20 msec/point provides a sweep duration of 20.48 seconds.

By observing figures 18,19,20 it is noted that an average of 15 small amplitude events occur prior to the large amplitude "extension" event which has a characteristic decay time of 60 msecs. The small

amplitude events represent the elastic energy released during the propagation of the unilateral fracture through the zone of compressive radial stress

c) Model III

In this model a unilateral fracture is propagated towards a region of very high compressive radial stress. Initially a bilateral fracture is initiated such as in model I and is in turn unilaterally propagated towards a heated zone.

The velocity of propagation of this unilateral fracture is observed to decrease significantly on close approach to the zone of compressive radial stress. This continuous deceleration is followed by an apparent momentary stopping of the propagation and a sudden bending of the propagation path at an angle of 45°. The direction of this bending coincides with the direction of maximum tensile hoop stresses.

The resulting bending fracture is approximately 6 cm long and the duration of propagation is roughly 40 seconds. Figures 21,22,23 show the acoustic emission activity associated with this propagation. The sampling rate of 50 msec/point provides a sweep duration of 51.20 seconds.

By observing the above figures it is noted that an average of 10 relatively large amplitude events, when compared to model II, precede the large amplitude bending event which has a characteristic decay time of 80 msecs. It is noted that more elastic energy is radiated in the form of large amplitude acoustic emissions in this model. It is therefore believed that the high compressive radial stress applied at the tip of this particular fracture is the cause of the large

amplitude precursory events. The absence of smaller amplitude events may be explained by the sampling interval being too large and thus missing short decay time events.

FIGURE 18: ACOUSTIC EMISSION ACTIVITY
FOR MODEL II.

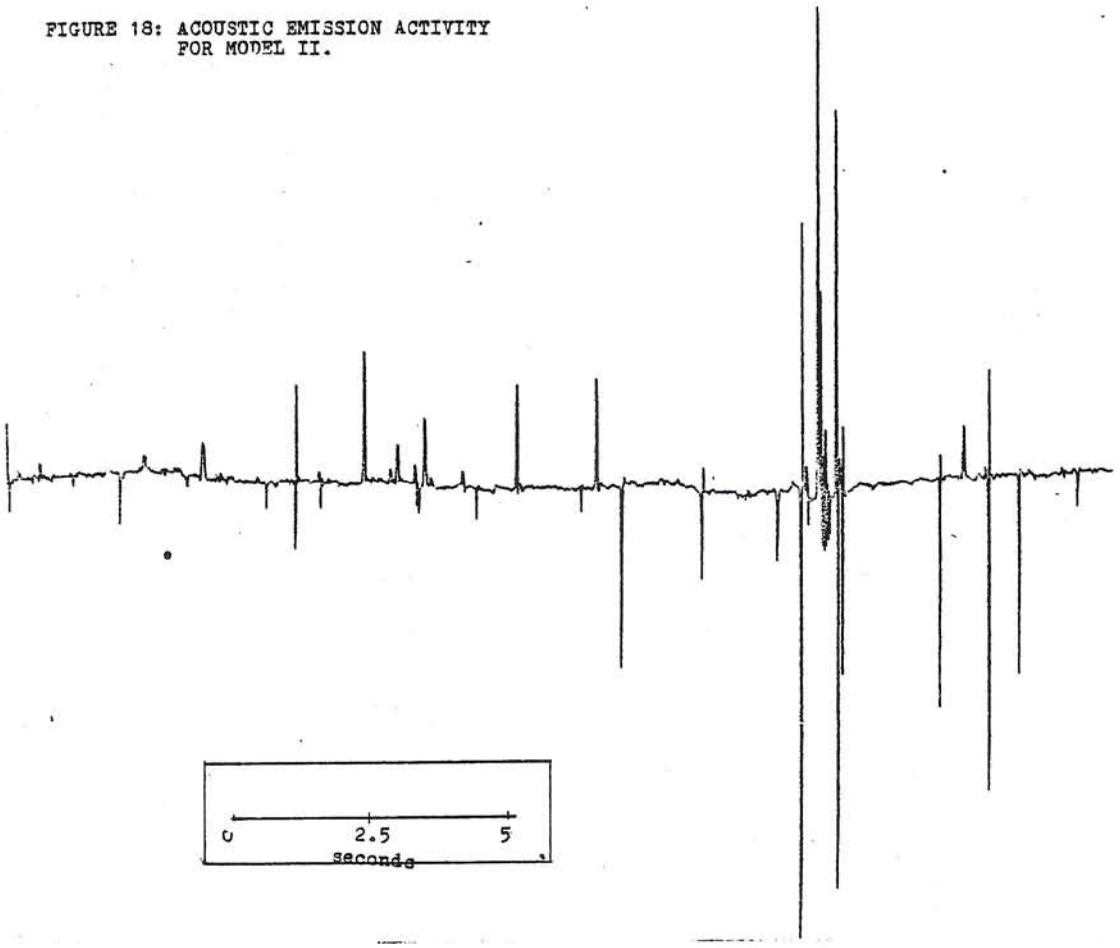

FIGURE 19: ACOUSTIC EMISSION ACTIVITY
FOR MODEL II.

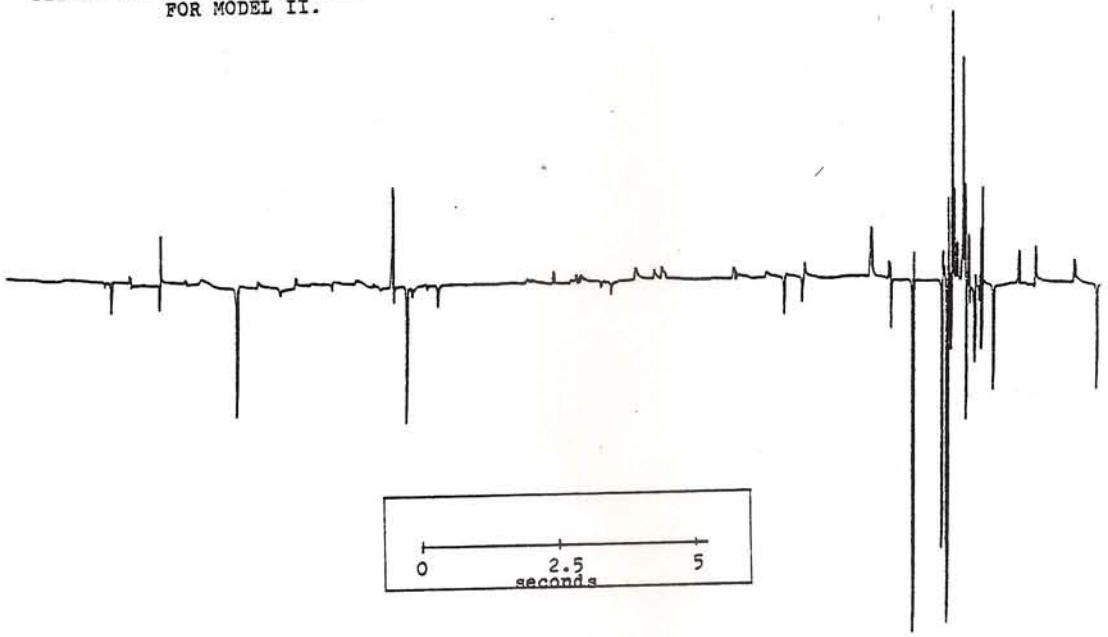

FIGURE 20: ACOUSTIC EMISSION ACTIVITY FOR MODEL II.

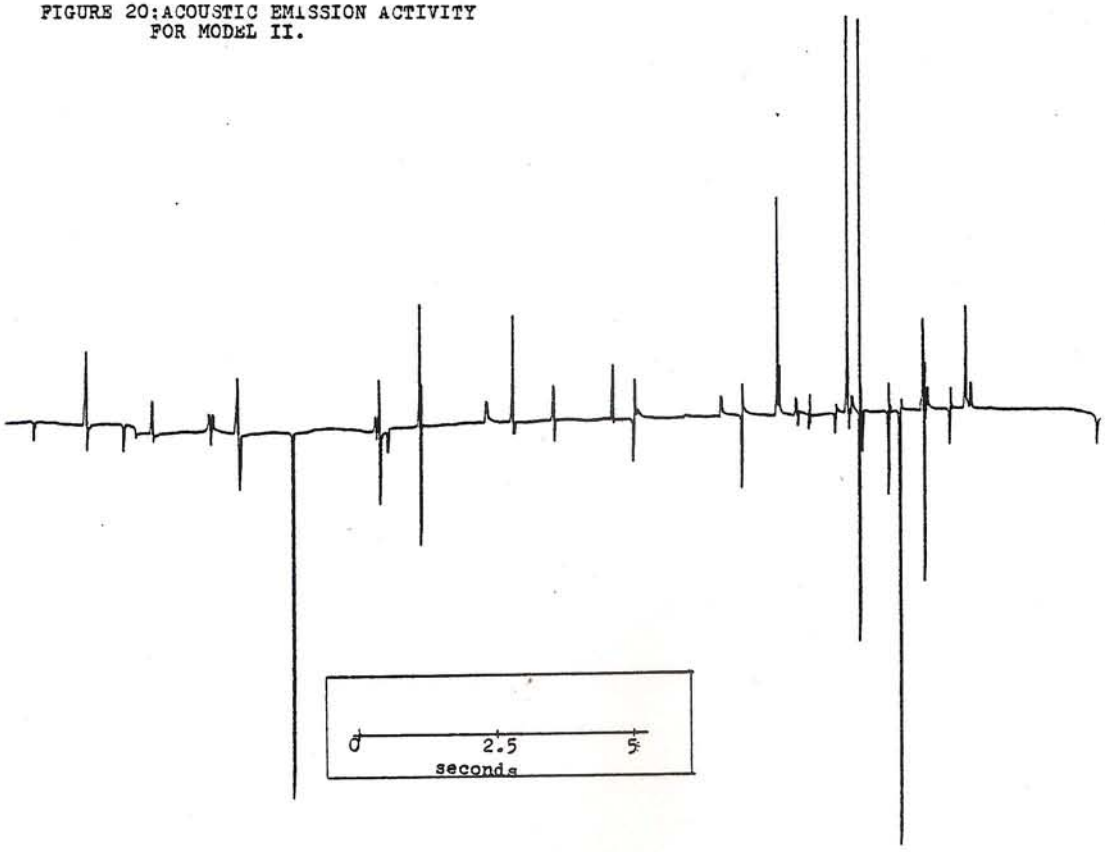

FIGURE 21: ACOUSTIC EMISSION ACTIVITY
FOR MODELL III.

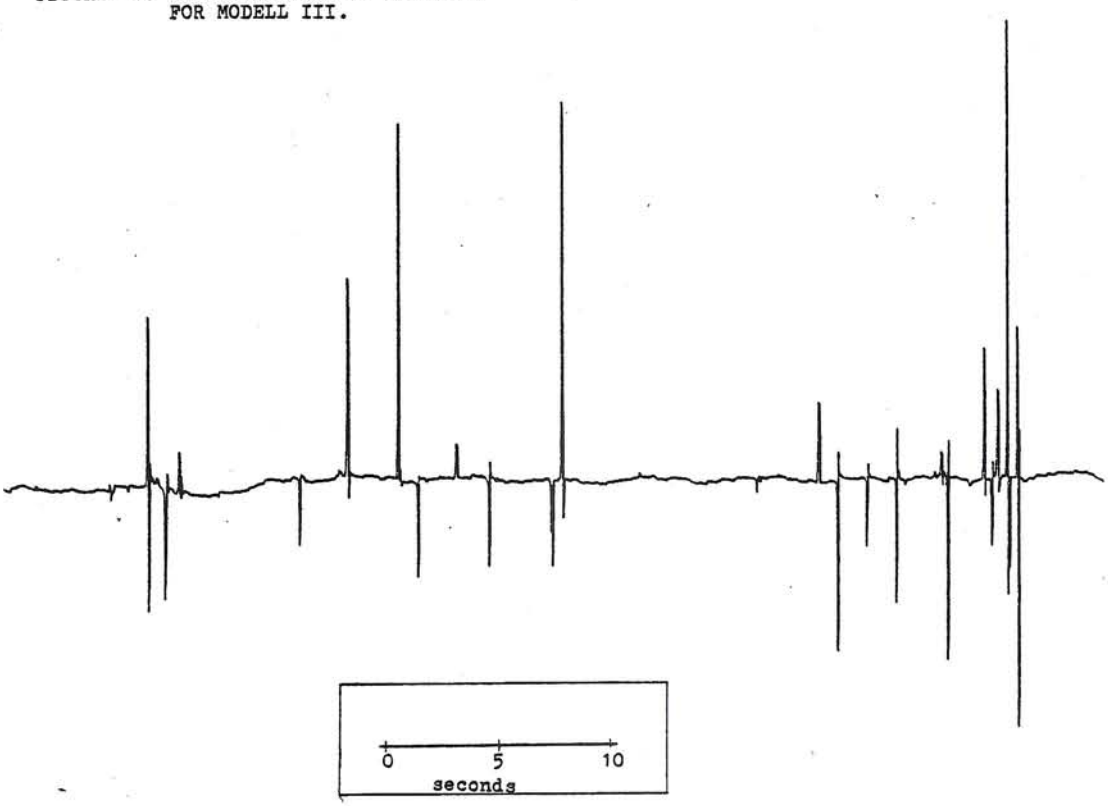

FIGURE 22· ACOUSTIC EMISSION ACTIVITY
FOR MODELL III.

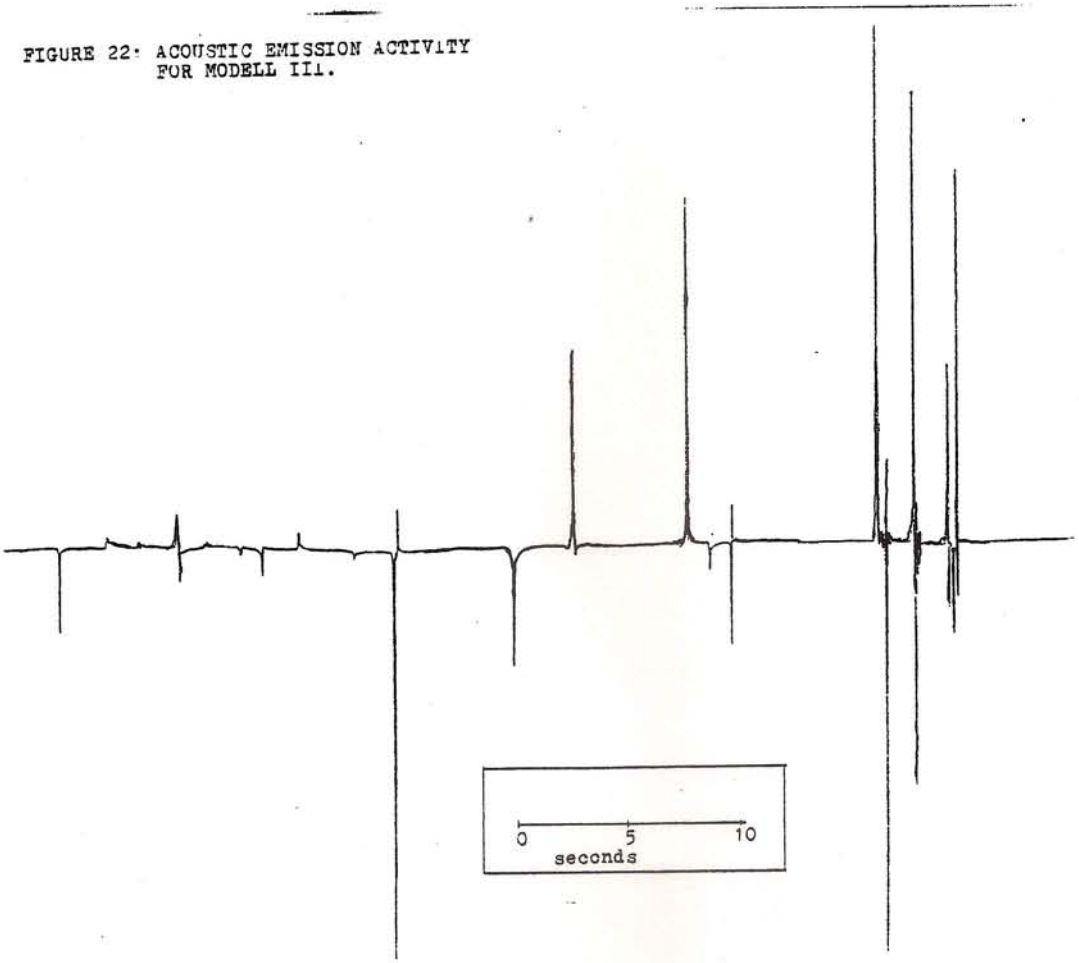

FIGURE 23: ACOUSTIC EMISSION ACTIVITY
FOR MODELL III.

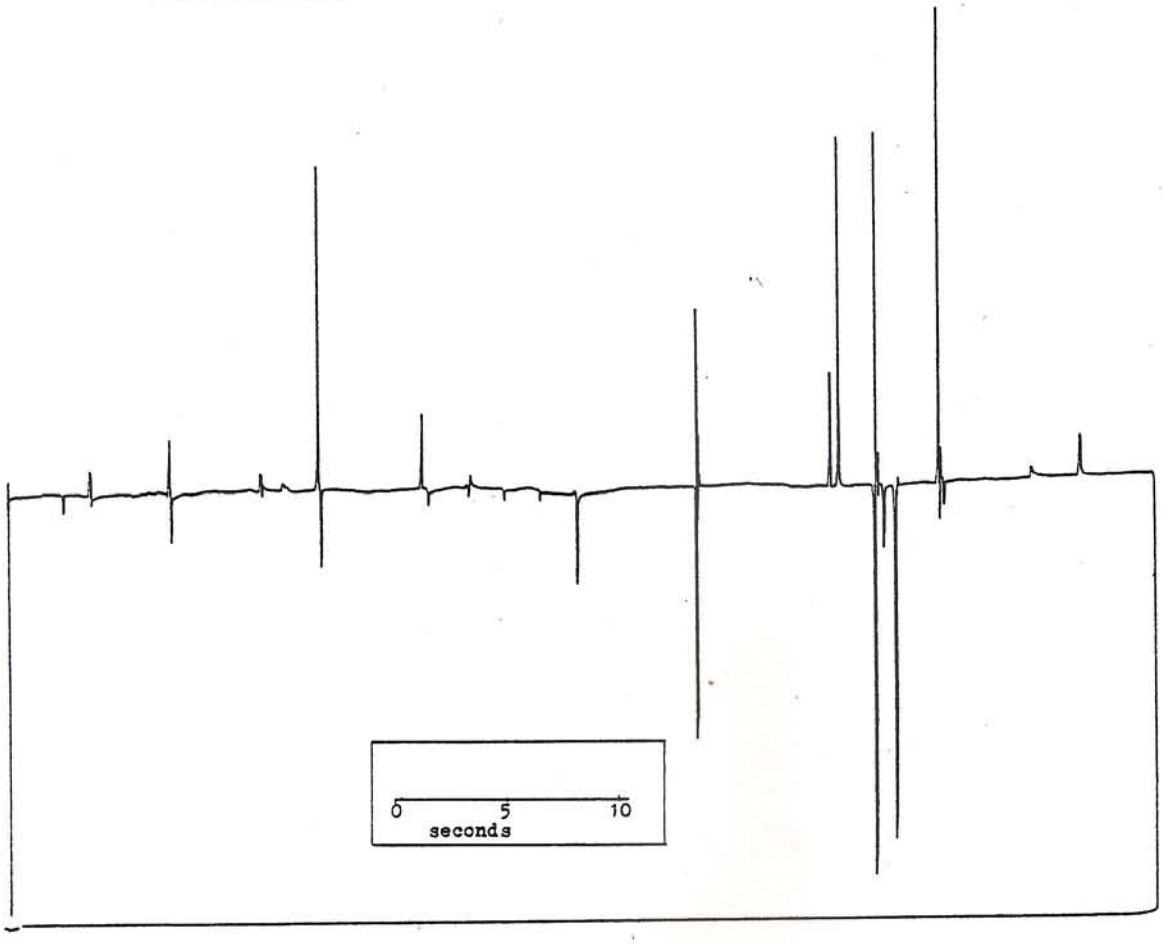

5) DISCUSSION OF RESULTS AND CONCLUSIONS

i) Discussion of results

The analysis of results in the previous section indicate a dependence of the amplitude and frequency of occurrence of the acoustic emissions to the stress distribution at the fracture tip. This same factor seems to control the velocity of propagation of the fracture.

In model I the tensile hoop stress at the centre of the preinscribed scratch is much larger than the compressive radial stress at the ends of the scratch and thus the formation of the bilateral fracture appears spontaneous. In this case the rate of crack formation and extension within the preinscribed scratch plane prior to the fracture formation may be too fast to be detected with the sampling rate available by the Nicolet oscilloscope. Another factor which may explain the lack of recorded precursory emissions in this model is the high trigger threshold level which does not allow any small amplitude events to be detected prior to the opening of the fracture wall.

In order to employ a lower trigger threshold level the false triggering by electromagnetic noise must be minimized or completely eliminated. A detector which has minimized the problem of random noise has been designed and is described in appendix II. A method of eliminating the false triggering by electromagnetic noise involves the separate triggering of each channel of a detecting array arranged assymetrically about the source location. Since electromagnetic noise will trigger all the channels simultaneously we may distinguish and reject the signals caused by it.

Further on, the errors involved in the localization of these events may be also minimized by the assymetrical distribution of more than two detectors about the line containing the preinscribed scratch.

In models II and III the presence of high compressive radial stress at the tip of the propagating fracture is observed to effectively induce a deceleration in the velocity of propagation as well as provide the fracture with energy to be released in the form of acoustic emissions precursory to a large amplitude event.

It is noted that the ampliutde of the acoustic emissions is larger in model III when compared to model II. The high compressive radial stress applied at the tip of the fracture in model III is the probable reason for this greater release of elastic energy.

However the results obtained in models II and III are subject to a few criticisms. First, an assumption is made with regards to the location of the acoustic emissions recorded. These acoustic emissions are assumed to occur within the plane of the propagating fracture. This assumption is based on experimental results which localize only the initiation of the fracture and show that deformation is initiated within the preinscribed scratch plane. It is therefore believed that deformation will continue only in that plane. Next the analysis of the relative amplitudes of the acoustic emissions in the three models is subject to errors due to the fact that we are not entirely sure which part of the burst-type emission signal is sampled. In order to arrive at the above relation between amplitudes of signals and stress distribution many experiments were performed for each model and the overall observed pattern is stated as the result.

An important consideration in the orientation of the detecting array with respect to the source is the radiation pattern of the acoustic emissions. In the design of the detecting array orientation for this experiment, it was assumed that the radiation pattern is that of an extensional dislocation. It should be noted however that certain bending stresses may well exist due to the heating of only one side of the glass surface. These bending stresses are more likely to produce shear deformation in regions where the fracture tip approaches the thermally stressed zone. As a result the further investigation of source mechanisms is necessary in future modelling studies.

Since crack formation and extension are the likely mechanisms generating the acoustic emission signals recorded in this investigation, the identification of their characteristic signals in time and space may prove valuable in source migration studies involving propagating tensile fracture models.

CONCLUSIONS

ii)

The results from this study verified the existence of acoustic emission patterns precursory to the formation of 3 types of tensile fractures.

The rate of occurrence, and the amplitudes of the observed patterns are shown to be dependent on the nature of applied stress field as well as on the velocity of propagation of the fracture.

It is thus deduced that acoustic emission patterns observed in controlled modelling experiments involving fractures in glass, are analogous to precursory seismicity patterns. Thus the application of sophisticated instrumentation in detecting and localizing these acoustic emissions may prove beneficial in source-mechanism and source-migration studies.

APPENDIX I

LOCALIZATION OF ACOUSTIC EMISSIONS USING TWO DETECTORS

The geometry of the problem is shown in figure 24. Given the time difference (Δt), of an emitted p-wave travelling with a velocity (V), at two detectors, we wish to locate the source along a line perpendicular to the detecting array.

Figure 24 :
Geometry of localization problem.

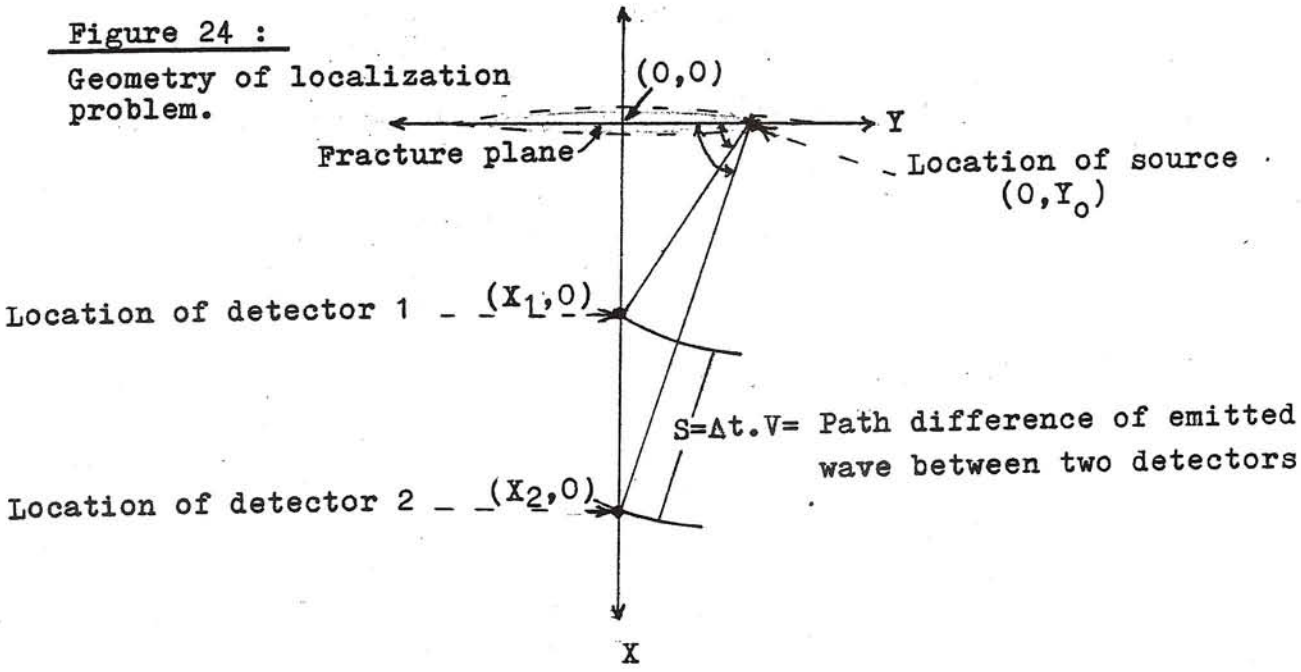

From simple geometry it may be shown that :

$$S=(X_2^2+Y_o^2)^{1/2} - (X_2^2+Y_o^2)^{1/2}$$

Squaring both sides twice and solving for Y_o we obtain:

$$Y_o = \left[\frac{(S^2-X_2^2-X_1^2)^2-4X_2^2X_1^2}{4S^2}\right]^{1/2}$$

This method provides a twin solution $\pm Y_o$, on either side from the centre (0,0) of the fracture.

APPENDIX II

DESIGN OF A LOW NOISE ACOUSTIC EMISSION DETECTOR

The principle aim of this design is an acoustic emission detector which exhibits good sensitivity to a wide range of signals, low noise and good coupling with any flat surface.

During the course of investigating acoustic emission signals in glass plates, it was noted that the bimorph type piezoelectric crystals provide adequate sensitivity to the emitted stress waves. It was also noted that the reception of the signals was considerably enhanced by the presence of a thin coupling layer of liquid silicone, between the crystal and the glass surface. The major problem encountered with the detector design employed in that study was the presence of electromagnetic noise in the amplified signal. This noise was observed to be considerably reduced by making the leads connecting the piezoelectric crystal to the amplifier very short. In practice though it was necessary to have leads as long as 20 cm and thus shielded cable was employed and appeared to eliminate some of the noise present in the amplified signal.

In this current detector design the problem of electromagnetic noise is essentially eliminated by positioning a miniature operational amplifier circuit next to the piezoelectric crystal and enclosing the system in a plastic casing (see figure 25).

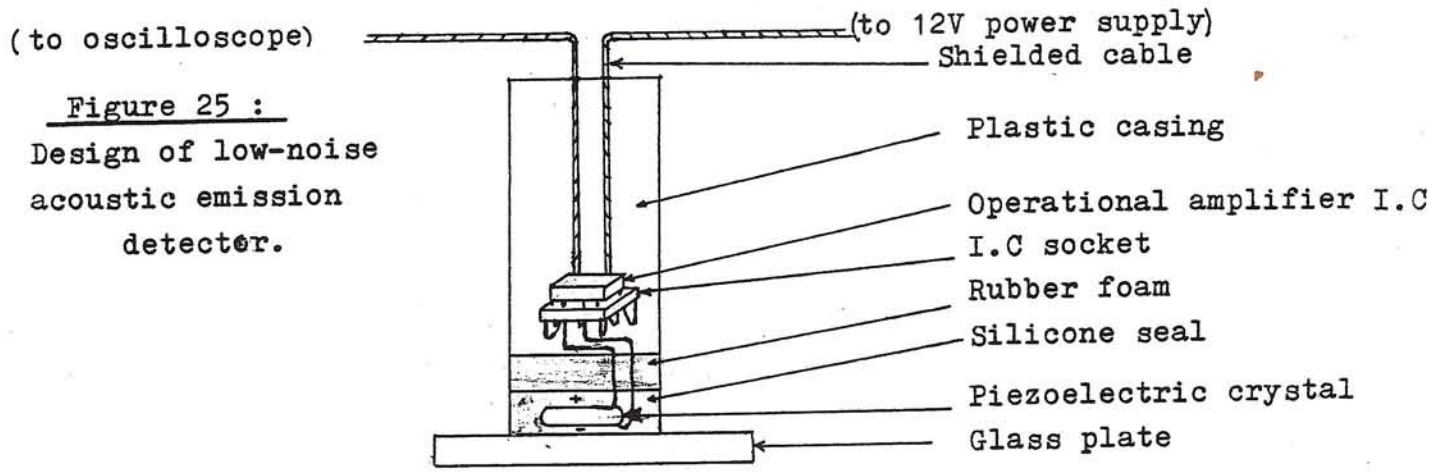

Figure 25 :
Design of low-noise acoustic emission detector.

The detecting piezoelectric crystal employed is of the bimorph type in the shape of a disk. The direction of maximum sensitivity of this disk is in the thickness mode. Lead output wires are soldered on each side of the disk and also to the input resistances of an operational amplifier circuit. The length of these leads must be a minimum (2 cm). The input, output and feedback resistances of the operational amplifier circuit are soldered on a 8 pin socket to prevent the amplifier chip from overheating. Once these connections are proven to be continuous in their electrical contact, the amplifier chip is mounted in the socket. The proper selection of input and feedback resistances provides one with the desired gain. The slew rate of the amplifier must be chosen to be responsive very quickly to an incoming high frequency signal. Also the bandwidth must provide equal gain for the desired frequency range.

In this design a high-slew rate(50v/μsec), wide bandwidth (1MHz) operational amplifier is employed, providing the signal a gain of 100 over its original amplitude. This amplifier is operated from a 12 volt power supply which is connected to the 8 pin socket by shielded cable. The system has two external leads, one to the power supply and one to the input of an oscilloscope.

Once all the soldering is completed, the operational amplifier circuit is put into a 1" x 4" tube shaped mould. Care is taken to keep the piezoelectric crystal outside this mould as well as having the external leads coming out from the other side of the mould. This mould is filled with liquid plastic and allowed to dry for 12 hours. The mould is then removed and the piezoelectric crystal is mounted on a foam rubber backing which rests against the liquid plastic casing. The crystal is held together with the foam backing onto the end of the liquid plastic rod by means of a silicone seal enclosure. The end of the crystal which is to be used in contact with a flat surface has a very thin layer of silicone seal compared to its sides and back.

This detector design has proven to detect very clean, low noise signals and is to be applied in further acoustic emission modelling experiments.

REFERENCES

Dmowska, R. and Li, V.C. (1981). Asperity model for precursory seismicity patterns for some large earthquakes. IASPEI 1981 Abstracts A 4.3.

Egle, D.M, Tatro, C.A. (1966). Analysis of acoustic emission strain waves. The Journal of the Acoustical Society of America. v 41, # 2, pp 321-327.

Griffith, A.A. (1920). Phenomena of rupture and lfow in solids. Trans. Roy. Soc. (Lond.), Series A, 221, pp 163-198.

Inglis, C.E. (1913). Stress in a plate due to the presence of cracks and sharp corners. Trans. Inst. Naval Arch., 60, pp 219-231.

Irwin, G.R. (1957). Analysis of stress and strains near the end of a crack. J. Appl. Mech, 24, 361.

Irwin, G.R. (1960). Fracture mode transition for a crack traversing a plate. J. Basic Energy. pp 417-425.

Irwin, G.R. (1966). Crack propagation behaviours. Expt 1. Mech. pp 321-330.

Kaiser, J. (1950). "Untersuchengen uber das Auftreten von Gerauschen geim Zugversuch". Ph.D. Thesis, Technische Hochschule Munchen, Germany.

Keilis-Borok, V.I., Knofoff, L. Rotvain, I.M. (1980). Bursts of aftershocks, long-term precursors of strong earthquakes, Nature, 283, pp 259-263.

Kostrov, B.V. and Das, S. (1981). Idealized models of fault behaviours prior to dynamic rupture. IASPEI 1981. Abstract 4.15.

Licht, T. (1979). Acoustic Emission. Bruel & Kjaer, Technical Review, 2, 1979.

Mansinha, (1964). The propagating fracture of constant shape. J. Mech. Phys. Solids, 12, pp 333-360.

Mogi, K. (1962a). Study of elastic shocks caused by the fracture of heterogeneous materials and its relation to earthquake phenomena, Bull. Earthquake Res. Inst., Tokyo Univ., 40, pp 125-173.

Mogi, K. (1962b). On the time distribution of aftershocks accompanying the recent major earthquakes in and near Japan. Bull. Earthquake Res. Inst., 40, pp 107-124.

Mohanty, B.B. (1969). Ph.D. Thesis Toronto.

Oliver, J., Press, F. and Ewing, M. (1954). Two dimensional model seismology, Geophysics, 19, pp 202-219.

Rindorf, H. J. (1981). Acoustic emission source location in theory and in practice. Bruel & Kjaer, Technical Review 2, 1981.

Savage, J.C. and Mansinha, L. (1963). Radiation from tensile fracture. J G R, 68, pp 6345-6358.

Scholz, G.H. (1968a). Microfracturing and the inelastic deformation of rock. J. Geophys. Res. 73, pp 1417-1432.

Scholz, G.H. (1968b). An experimental study of the fracturing process in brittle rock. J. Geophys. Res. 73, pp 1447-1454.

Van Vlak, L.H. (1973). A textbook of materials technology. Addison Wesley.